CONF-851125--15

HYPOTHETICAL ACCIDENT SCENARIO ANALYSES FOR A 250-MW(T) MODULAR HIGH TEMPERATURE GAS-COOLED REACTOR*

R. M. Harrington S. J. Ball J. C. Cleveland

Oak Ridge National Laboratory

Oak Ridge, Tennessee 37831

CONF-851125--15

TI86 002179

ABSTRACT

This paper describes calculations performed at Oak Ridge National Laboratory, under the auspices of the U.S. Nuclear Regulatory Commission's HTGR Research Program, to characterize the inherent safety of a 250-MW(t), 100-MW(e), pebble bed modular high temperature gas-cooled reactor (HTGR) design with vertical in-line arrangement (i.e. upflow core with steam generators directly above the core). A variety of postulated accident sequences involving combinations of loss of forced primary coolant (helium) circulation, loss of primary coolant pressurization, and loss of heat sink were studied and are discussed.

1. INTRODUCTION

MASTER

Licensing and public acceptance problems besetting the current generation of light water power reactors have renewed interest in reactor concepts with greater inherent safety. Small HTGRs under study

*Research Sponsored by the Office of Nuclear Regulatory Research, U.S. Nuclear Regulatory Commission, under Interagency Agreement DOE-40-551-75 with the U.S. Department of Energy under contract DE-AC05-84OR21400 with Martin Marietta Energy Systems, Inc.

DISCLAIMER

by the U.S. Department of Energy have been proposed as fitting into the inherently safe category. This paper describes computer code development and accident sequence calculations performed at ORNL, under the sponsorship of the USNRC HTGR safety research program, to establish essential features of postulated heatup accidents of the 250-MW(t) modular HTGR. This paper describes work on "vertical in-line" (VIL) design, so called because the steam generator is located directly above and in vertical alignment with the reactor core. Both the core and steam generator are housed within a single steel pressure vessel.

Three different computer codes are discussed in this paper. The first code, described in Sect. 2, has multi-node reactor core, reflector, and reactor vessel models and in addition calculates the primary coolant circulation and pressure and heat transfer to the steam generators. This code is applied, in Sect. 3, to calculate the peak and average fuel and reactor vessel temperatures during hypothetical heatup accidents initiated by loss of forced circulation (LOFC) of the primary coolant. The LOFC accidents considered here involve the simultaneous and permanent failure of all the helium circulators. Results are also presented for sequences in which the LOFC accident is further complicated by concomitant loss of steam generator cooling and/or loss of primary coolant pressurization.

The second computer code (Sect. 4) utilizes similar programming techniques to model the 46-MW(t) Arbeitsgemeinschaft Versuchs Reaktor (AVR) in Juelich, West Germany. This reactor has many features similar to the VIL modular designn. The code is applied to simulate the effect of a large reduction in primary coolant flow without intervention by the reactor protection system. The results compare favorably to the actual plant data, demonstrating an important safety characteristic of the small HTGR.

The third computer code is presented in Sect. 5. This code has simplified core and reactor vessel heat transfer models, but detailed thermal models of the reactor vessel cavity, liner, concrete wall, and surrounding earth (bedrock). The code is programmed to calculate the fuel, reactor vessel and reactor cavity temperatures that would occur if the worst case heat-up accident postulated in Sect. 3 were further complicated by the long-term loss of the reactor cavity cooling system. Such accident sequences are very unlikely due to the passive features of the cavity cooling system and due to the extremely long times involved in such heatups (typically 2 weeks to 6 months). Results are discussed in Sect. 6.

Tentative conclusions with respect to basic safety features of the modular HTGR are briefly considered in Sect. 7.

2. MODEL FOR HEATUP AFTER LOFC

The reference model used for the pebble bed core and graphite block side reflector is a two-dimensional (R-Z) representation that includes both radial and axial conduction. Convection cooling by the primary system helium is assumed to occur in the pebble bed core but not in the reflector. In the nodal structure each axial segment has three radial nodes for the pebble bed core, two for the side reflector, and one for the core barrel wall (Fig. 1). In a more detailed core model used for sensitivity studies, six radial nodes were used for the pebble bed core. There are ten axial segments. The radial core flow distribution is assumed to be uniform, and the total flow (if nonzero) is always assumed to be in the normal (upward) direction. A capability for modeling reverse (downward) flows would be useful only for simulating cases where slow leaks occurred near the bottom of the pressure vessel. The convective cooling model uses an exponential approach algorithm for computing coolant gas temperature, which permits representation of very low flows. The model of the graphite top reflector calculates internal convective heat transfer from the primary coolant and radiative heat exchange with the top surface of the core.

The core pebble bed and reactor features were assumed to be those of a 1984 GA Technologies (GAT) plant design, with primary system characteristics as shown in Table 1. Physical property data and correlations were taken from current sources applicable to pebble bed technology. Helium convection heat transfer uses the Jeschar correlation (Ref. 1); pebble bed core effective conductivity is derived from Breitbach and Barthels (Ref. 2); core specific heat uses a correlation by Petersen (Ref. 3); and the afterheat curve is from a KFA correlation (Ref. 4). Data published by GAT (Ref. 5) was used for side reflector thermal conductivity, with higher thermal conductivity assigned to the relatively unirradiated outer 50 cm of the 100 cm thick reflector.

The temperature of the core barrel and reactor vessel is calculated for each of 10 axial regions in the core model. The 2.54-cm-thick core barrel is in contact with and receives heat by conduction from the outer reflector of the core. The core barrel and reactor vessel are separated by the coolant downcomer annulus. The surface of the reactor cavity is assumed to be maintained at 150 C to represent the condition of the cavity cooling system operating in the passive (i.e., natural convection) mode.

A steam generator model is provided to complete the calculation of primary coolant temperatures throughout the primary coolant system. The present steam generator model is very rudimentary but is equipped with two modes to allow the simulation of either continued feedwater flow or the loss of all feedwater flow. For the mode that simulates continued feedwater flow, the helium is assumed to exchange heat with metal tubes that are at a single uniform temperature. The metal temperature is an input parameter and is assumed to be maintained constant by the continued flow of feedwater. The mode that simulates the loss of feedwater treats the steam generator tube metal as a passive heat sink that exchanges heat with the incoming helium.

After the loop temperatures are calculated, the constant-inventory reactor vessel pressure is calculated by volume-weighting the inverse absolute temperatures throughout the primary coolant loop. For transients involving loss of helium inventory (depressurization), the current model bypasses the pressure calculation and accepts an input pressure vs time profile.

The natural circulation flow rate of helium during an LOFC accident depends on the driving head caused by the helium density differences around the loop and on the total pressure drop due to the temperature differences in the primary coolant flow circuit. Since all coolant within the vessel is at essentially the same pressure, the density differences are due to temperature differences in the primary coolant flow circuit. A total unrecoverable pressure drop of 0.137 MPa (20 psi) at full power was used for the helium circuit. To relate this known total pressure drop to the unknown total pressure drop at reduced flows, the "smooth pipe" assumption was employed: the friction factor is proportional to the −0.2 power of Reynolds number (or mass flow).

3. RESULTS: LOFC ACCIDENTS

An extreme variation of the worst-case LOFC accident is a reactor scram followed by simultaneous loss of primary system pressure, along with a loss of feedwater cooling to the steam generators (Fig. 2). In this case the maximum fuel temperature reached 1549 C at 21 h from the start of the transient. Maximum pressure vessel temperatures were <315 C. Average steam generator tube metal temperature peaked at 704 C within the first hour. The steam generator tubes at the top (primary coolant inlet) end would reach higher temperatures because they are the first to be exposed to the hot helium drafting upward from the core (peak coolant temperature at steam generator inlet was 911 C at 30 h). The single-node steam generator model calculates the average tube temperature but provides no estimate of the temperature of the hottest tubes.

The small amount of primary system natural circulation flow (0.05 kg/s or 0.05%) was marginally effective in reducing the maximum fuel temperatures, as evidenced by the fact that in a run in which the flow was forced to zero, the maximum fuel temperature reached 1599 C at 22 h. The time spent at the higher temperatures was also longer for the no-flow case.

In a second variation, it was assumed that forced circulation was lost and the system depressurized, but the feedwater to the steam generators was maintained. This led to a slight reduction in the maximum fuel temperature by virtue of the slightly increased natural circulation (0.08 kg/s). Here, the maximum fuel temperature of 1487 C occurred at 19 h. Naturally, the steam generator temperatures were reduced considerably, remaining below the normal operating values after the start of the transient. Maximum pressure vessel temperatures in the core region were also lower (<253 C).

In a third, more realistic case, it was assumed that the system remained pressurized, with LOFC and loss of feedwater flow to the steam generators occurring at time zero (Fig. 3). The natural circulation flows are much larger here (0.7 to 1.0 kg/s), and the core cools relatively rapidly. The maximum fuel temperatures are only about 70 C greater than the normal operating values. The pressure vessel temperature does get higher than in the other cases, however, due to the higher flow rates during the cooldown and reaches 410 C, 8 h into the run. The average steam generator tube temperature (approximately equal to the steam generator outlet temperature on Fig. 3) reaches a maximum of 745 C at 1.5 h. Tubes at the steam generator inlet would more closely approach the hot leg outlet temperature, which peaks at 817 C after 0.5 h.

Calculations were made to test the sensitivity of the results to model assumptions and input data. The peak fuel temperature after a depressurized LOFC accident with coincident loss of steam generator cooling was used to quantify the effect of each change. For example, a run was made in which the heat transfer from the exterior of the reactor vessel was arbitrarily held at zero. The results contradict intuitive expectations. The peak fuel temperature (occurring 24 h after accident initiation) was only 30 C higher for the case without any vessel heat loss. Of course, without any vessel heat removal, higher fuel temperatures would eventually be reached, but this would occur long after 24 h.

Sensitivity of peak fuel temperature to fuel and reflector thermal conductivity and to decay heat was also examined for the depressurized LOFC accident without steam generator cooling. A modified core thermal conductivity (i.e. effective heat transfer across the bed of fuel pebbles) correlation with about 10% higher conductivity in the 1300 to 1500 C region resulted in an approximately 50 C lower peak fuel temperature. A modified decay heat correlation with about 10% lower decay heat resulted in a 100 C reduction in predicted peak fuel temperature. Finally, the effect of side reflector conductivity was examined by using older, more conservative data for graphite thermal conductivity and by not taking advantage of the fact that the outer 50 cm of side reflector graphite is relatively unirradiated. These changes, which yield an approximately 50% lower average side reflector thermal conductivity, resulted in a predicted 130 C higher fuel temperature.

One potentially important "parameter" is the axial variation of heat generation within the core. The shape of the axial power profile is sensitive to the fuel management strategy employed. An axial profile with peak to average heat generator ratio of 1.7 was employed for the present work. A more highly peaked profile could result in higher fuel or reactor vessel temperatures.

4. COMPARISON TO AVR PLANT DATA

The AVR is shown in Fig. 4 and technical information is summarized in Table 2. The core is fueled with 6-cm diameter graphite pebbles containing coated fuel particles. During operation, pebbles are continuously withdrawn from the bottom of the reactor core and pebbles are added at the top.

Helium flows upward through the pebble bed and then across the steam generator tubes to produce steam. The reactor can operate at full power with a gas outlet temperature ranging from 770 C to 950 C. The steam generator is located above the core in the steel reactor vessel. It is shielded from core radiation by a 50-cm-thick graphite top reflector and two blowers located in the lower part of the vessel. The power of the reactor is controlled by varying the coolant flow. The AVR has four control rods that are utilized to control the core coolant outlet temperature and to achieve cold shutdown. The control rods were held stationary during the tests discussed here.

To examine reactor response to large flow reductions, ORNL is analyzing selected experiments from a series of tests performed at the AVR during 1982–1983. The AVR staff performed these tests to examine the change in reactor performance as the core composition was changed from all HEU/Th core to mixed HEU/Th and LEU core.

The approach used in the modeling is to first use fairly simple models to examine various effects, then improving the modeling detail as necessary. Model features are summarized below:

- space independent neutron kinetics with six groups of delayed neutron precursors.

- a coarse-structure thermal model with heat conduction dynamics and heat convection in each axial section approximated by a model of the "average pebble" in that section.

- nuclear importance (flux squared) weighting of solid temperatures in the axial direction to determine the effective temperature-to-reactivity feedback.

- computation of reactivity effects due to changing Xe-135 concentration using coupled equations for the core average iodine and Xenon concentrations based on the core average thermal flux level.

- a quasi-static, one-dimensional representation of the helium temperature and flow.

- for forced convection conditions, helium flow is computed from measured circulator speed, core inlet temperature and pressure assuming volumetric flow is proportional to speed. For natural convection conditions, helium flow is computed by balancing unrecoverable losses through the primary loop against the density difference driving head.

- computation of the decay power contribution to total power as the output of a series of optimized lead-lag filters with prompt power as an input.

Figure 5 shows the calculated results and the measured power for a flow reduction test performed April 16, 1982. The reactor was initially at full power with a core inlet gas temperature of 271 C and a gas outlet temperature of 807 C. The test was initiated by reducing the speed of each circulator from 4000 rpm to 2000 rpm over 68 s. The speed was held constant at 2000 rpm until shutdown of both circulators was initiated at 1085 s. During the test there was no control rod motion. When the circulator speed was reduced, the large negative temperature coefficient and the increasing fuel temperature caused the power to closely follow the flow reduction. With the decrease in flux, the transient increase in Xenon concentration resulted in a negative reactivity contribution. About 150 s after the reduction in circulator speed, the core reactivity returned to zero with the negative contribution due to the increasing Xenon concentration being balanced by the positive fuel temperature contribution.

With shutdown of the circulators (initiated at 1085 s) the fuel heats up slightly, driving the reactor subcritical. Xenon concentration increases due to the decrease in burnout rate, and the resultant additional contribution of negative reactivity is sufficient to hold the reactor subcritical until the return to criticality at about 1600 s, even with cooling of the fuel by natural convection (which the model estimates to be about 8.5% of full flow, and which is confirmed by independent investigations by the AVR staff.

In summary, even with a 50% reduction in core flow and no control rod motion, the high heat capacity of the fuel and the negative temperature coefficient combine to produce only moderate changes (on the order of 30 C) in maximum fuel temperature.

5. MODEL FOR DISSIPATION OF DECAY HEAT TO EARTH HEAT SINK

Studies described in Sect. 3 covered depressurized heatup cases where the cooling system for the cavity cooling wall remained operative, either by forced convection cooling or by passive (boiling) cooling, following a depressurization and LOFC accident. This section describes the computer code developed for study of the longer-term reactor heatup problem that would evolve if the cavity-wall cooling is lost and if the ultimate heat sink is the earth surrounding the reactor vessel cavity. Dynamic solutions to this cylindrical geometry heat conduction problem were generated using the IBM Continuous System Modeling Program (CSMP) language's array integration feature that enabled, with little effort, a relatively fine-structure solution for the earth temperature history.

The total system model consists of a 2-node approximation of the reactor (average core and average side reflector), 1 node each for the reactor vessel and cavity concrete wall, and 50 radial (cylindrical-shell shaped) earth nodes. The parameters used for the effective heat capacity of, and conductance between, the core, side reflector, and reactor vessel were derived from the more detailed model described in Sect. 2. Modeling of the concrete liner heatup optionally assumes either no cooling or a limited supply of passive (boiling water) cooling. Neglect of axial temperature variation in the core and reactor vessel was shown (by using the code of Sect. 2) to result in an uncertainty of less than about 50 C. Neglect of axial conduction in the earth modeling is a conservative approximation. The outer radius chosen for the earth cylinder model ranged from 18.3 to 36.6 m for relatively short (500-h) transients to 107 m for the longer (3000-h to 1000-d) ones, the choice being a function of how far out the temperature perturbation penetrates. (The outer shell of the earth cylinder model is assumed to be insulated.)

6. RESULTS: DISSIPATION OF DECAY HEAT TO EARTH HEAT SINK

The accident sequence for the results presented in this section is initiated by a loss of forced primary coolant circulation, complicated by concomitant loss of steam generator cooling and loss of primary coolant pressurization, and further compounded by the loss of the reactor cavity cooling system. The consequences are discussed in terms of the maximum reactor vessel and cavity wall temperatures. As demonstrated in Sect. 3, the peak fuel temperatures are nearly independent of cavity wall and earth temperatures since they occur relatively early in the accident (first 24 h). In none of the cases of this section was there a secondary fuel temperature peak approaching in severity the magnitude of the initial (24 h) peak.

Figure 5 shows the temperature versus time of the reactor vessel for the four possible combinations of input assumptions of "low"/"high" thermal conductivity of the earth and of "low"/"high" reactor core afterheat generation. The "low" thermal conductivity is 0.9 w/mC (0.5 Btu/h-ft-F). Such a value would be typical for stone concrete or dry limestone. The "high" value of earth thermal conductivity is 2.9 w/mC (1.7 Btu/h-ft-F); this is based on measurements of the properties of limestone bedrock encountered during an existing earth heat removal experiment at ORNL (Ref. 6). The "low" afterheat generation is that used for the model in Section 2; the "high" afterheat is from a conservative correlation used for HTGR liciensing analyses (Ref. 7).

The four curves on Fig. 5 show that the consequences of permanent loss of liner cooling water after the worst-case LOFC accident can range from mild to severe. Curve 1 ("low" reactor afterheat and "high" earth thermal conductivity) has a relatively mild consequence since both the reactor vessel steel and the concrete wall of the vessel cavity could withstand the 373 C peak reactor vessel temperature. Concrete wall surface temperature, not shown, remains about 25 C below reactor vessel temperature throughout the accident. Curves 2 ("high" conductivity and afterheat) and 3 ("low" conductivity and afterheat) exhibit peak vessel temperatures over 573 C that could bring about undesirable changes in reactor vessel steel or cavity wall concrete; however, the basic structural integrity of either material would not be lost. The maximum consequences of the accident responses of Curves 2 and 3 would result in financial loss instead of a threat to public safety (financial loss considerations are beyond the scope of this paper).

The accident response of Curve 4 of Fig. 4 ("high" afterheat, "low" conductivity) would involve both financial loss and, possibly, compromised margins of public safety. The peak reactor vessel temperature is 1030 C, and the peak concrete temperature would cause degradation of both steel and concrete. The steel would suffer significant loss of strength; if buckling of the reactor vessel or its supports occurred this would violate the fixed-geometry assumption of this analysis. An assessment of chances of vessel or vessel support failure would require a stress analysis and possibly more detailed thermal analysis. The behavior of concrete at 1000 C is very dependent on the composition of the concrete; however, it would be reasonable to expect some surface crumbling and release of gaseous degradation products such as CO_2 and H_2O.

7. CONCLUSIONS

The modular HTGR plant appears to have, with respect to safety, desirable response characteristics following LOFC accidents. Even in the worst case LOFC with loss of primary coolant pressurization and loss of steam generator cooling, the maximum hot-node fuel temperature is limited to the neighborhood of the 1600 C design goal, and the core average temperature peaks below 900 C. Fuel damage in this temperature range should be minor. If steam generator cooling is maintained after a pressurized LOFC accident, the maximum hot-node and average fuel temperatures remain below normal full power values. If steam generator cooling fails early in a pressurized LOFC accident, damage to the steam generator tubes will result; an assessment of the degree of damage would require a detailed stress and thermal analysis of the steam generator response during the accident.

If the worst case LOFC accident must be analyzed for the case of extended loss of cavity cooling, then the heat dissipation to the surrounding earth must be considered in the analysis. Depending on site and reactor specific characteristics, the ultimate heat sink provided by the earth may or may not be sufficient to prevent severe consequences. The question of whether extended loss of cavity cooling must be considered in the design basis of modular HTGRs is beyond the scope of this paper.

REFERENCES

1. R. Jeschar, "Warmeubergang in Mehrkornschultungen aus Kugeln", Archiv fur das Eisenhuttenwesen, 35, 1964.

2. G. Breitbach and H. Barthels, "The Radiant Heat Transfer in the High Temperature Reactor Core After Failure of the Afterheat Removal Systems", Nucl. Technol. 49, 392-99, August 1980.

3. K. Petersen, "The Safety Concept of HTRs with Natural Heat Removal from the Core in Accidents", Juel-1872, October 1983.

4. W. Rehm, "Unterschungen uber die verzogerte Nachwarmeabfuhr bei einem Kugelhaufen-Hochtemperaturreaktor-Konzept grssber Leistung als Beitrag zu den Moglichkeiten der Begrenzung hypothetischer Unfalle",

Juel-1647, February 1980.

5. R. J. Price and L. A. Beavan, "Final Report on Graphite Irradiation Test OG-3", GA-A14211 (UC-77), GA Technologies, Inc., January 1977.

6. V. C. Mei and S. K. Fisher, "A Theoretical and Experimental Analysis of Bertical Concentric-Tube Ground-Coupled Heat Exchanges", ORNL/CON-153, Martin Marietta Energy Systems, Inc., Oak Ridge Natl. Lab., October 1984.

7. R. E. Sund, "Afterheat Calculations for HTGR", GA-LTR-4A, GA Technologies, Inc., July 1974.

Table 1. 250-MW(t) Modular HTGR Primary System Data

Reactor power, MW(t)	250
Power density, W/cm^3	3.7
Heat losses from NSS, MW(t)	3
Thermal power to NSS from circulators, MW(t)	4
NSS thermal power, MW(t)	251
Primary helium pressure, MPa (psia)	6.9 (1000)
Reactor inlet temperature, °C (°F)	255 (491)
Reactor outlet temperature, °C (°F)	687 (1269)
Number of helium circulators	4[a]
Helium circulator, ΔP, psi	20
Gas flow rate, kg/s (lb/h)	111 (881,820)

[a]Horizontal, single stage, axial compressor, external drive.

Table 2. Technical data for AVR

Thermal power rating, MW	46.0
Core power density, MW/m^3	2.5
Core inlet temperature, °C	275
Core outlet temperature, °C	950
Primary system pressure, bar	10.8
Core diameter, m	3.0
Steam pressure, bar	73
Steam temperature, °C	505
Absorber rods	4

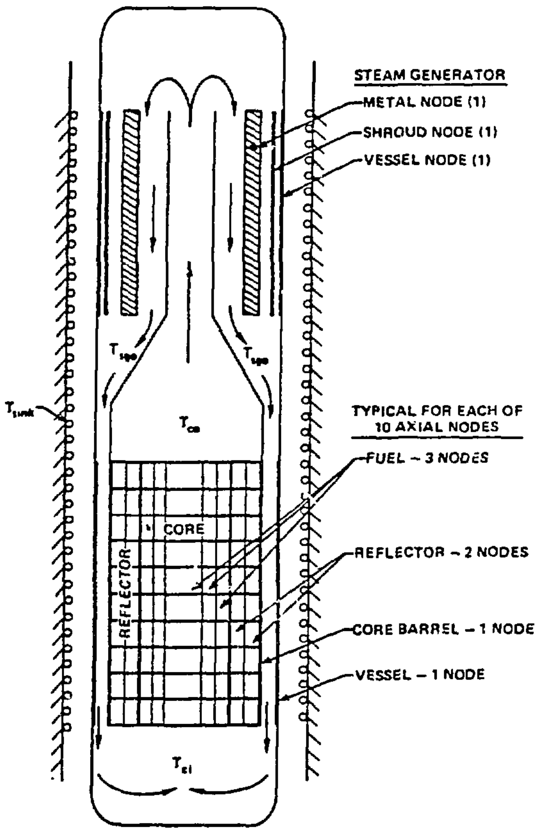

Fig. 1. Nodal structure of modular HTGR thermal model.

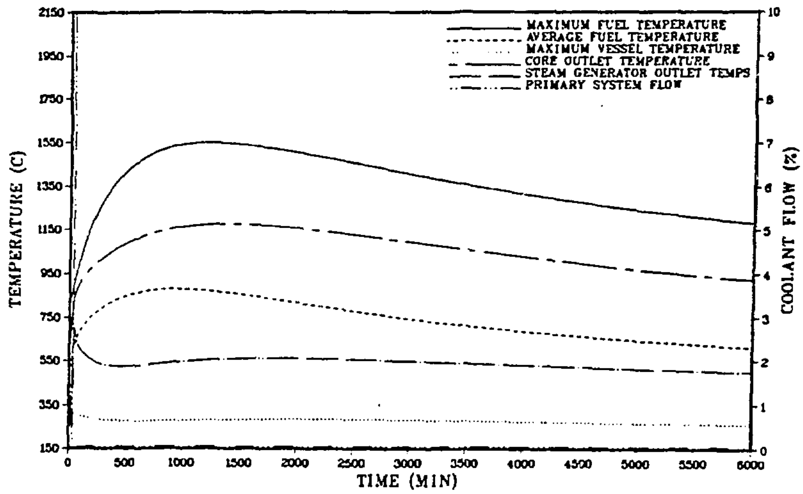

Fig. 2. LOFC with depressurization and loss of feedwater.

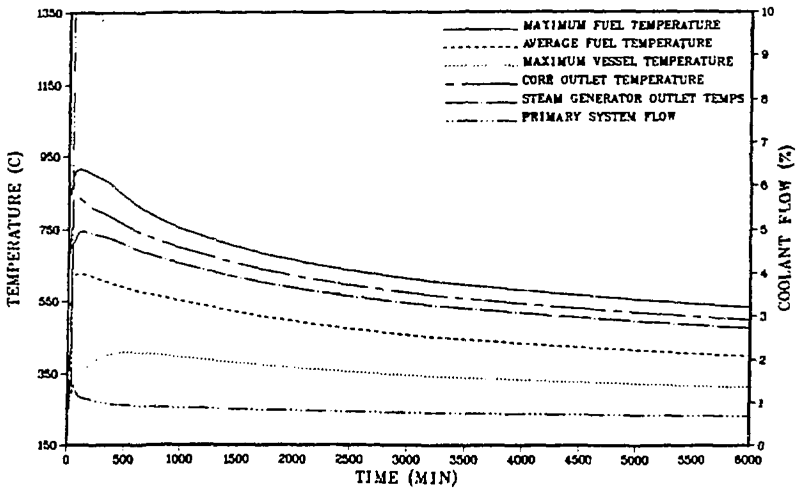

Fig. 3. LOFC with loss of steam generator cooling but without loss of primary coolant pressurization.

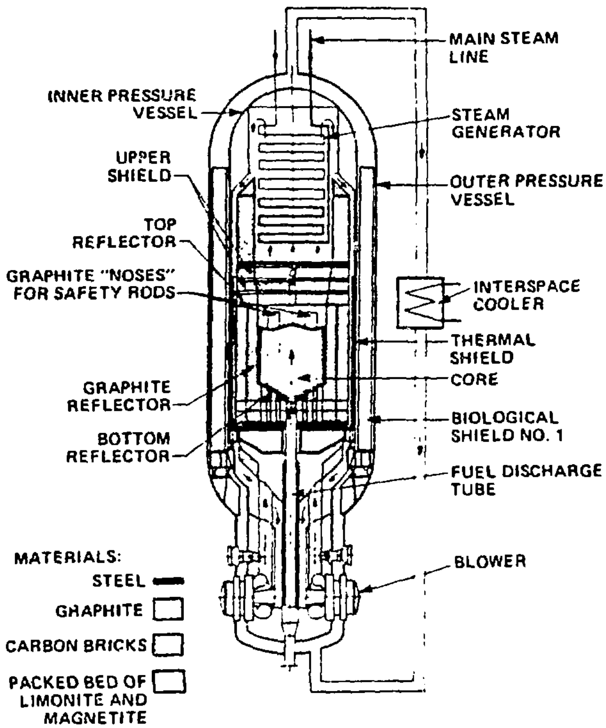

Fig. 4. AVR.

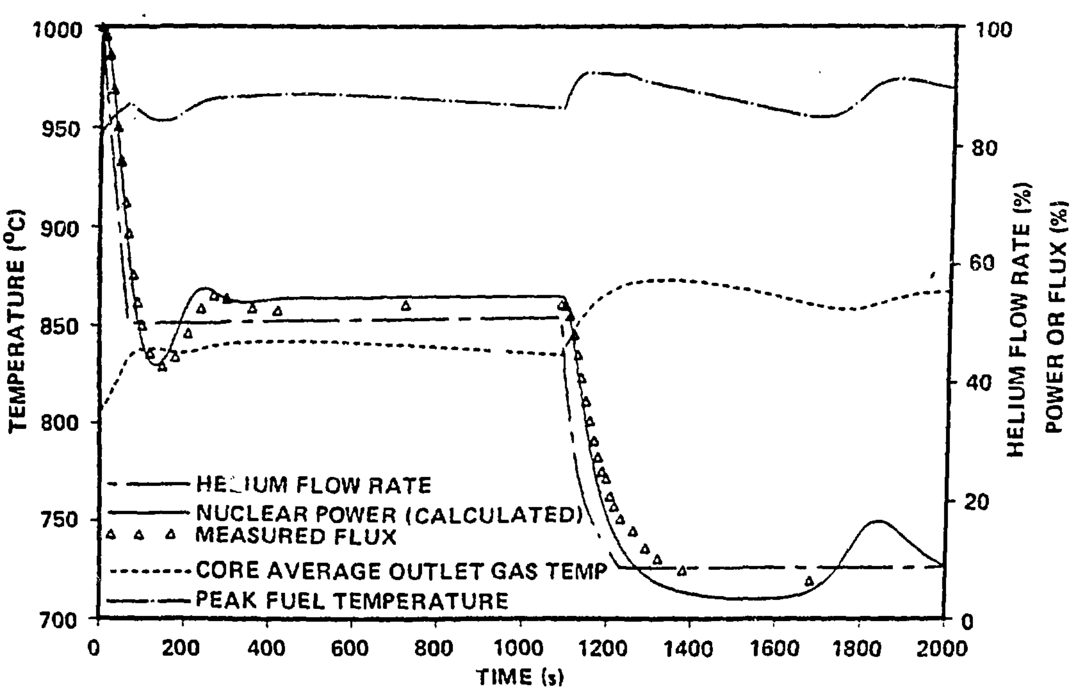

Fig. 5. AVR response to flow reduction of 4.16.82.

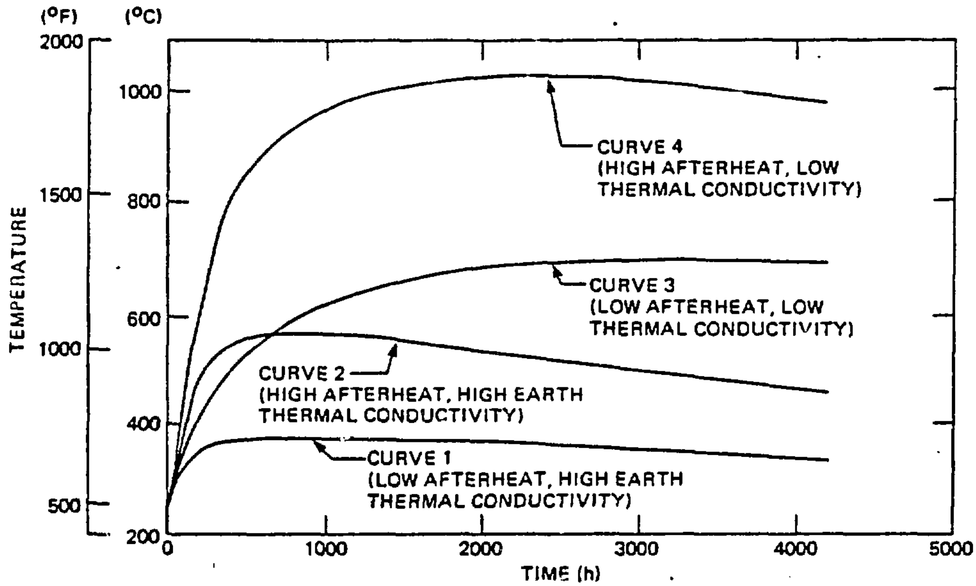

Fig. 6. Reactor vessel temperature after worst case LOFC accident with permanent loss of reactor cavity cooling.